# Critically coupled surface phonon-polariton excitation in silicon carbide

**Burton Neuner III,[1,*] Dmitriy Korobkin,[1] Chris Fietz,[1] Davy Carole,[2] Gabriel Ferro,[2] and Gennady Shvets[1]**

[1]*Department of Physics, University of Texas at Austin, Austin, Texas 78712, USA*
[2]*Laboratoire des Multimatériaux et Interfaces, Université Claude Bernard Lyon 1, 69622 Villeurbanne, France*
[*]*Corresponding author: bhn69@physics.utexas.edu*

Received June 2, 2009; accepted July 17, 2009;
posted August 4, 2009 (Doc. ID 112233); published August 28, 2009

We observe critical coupling to surface phonon-polaritons in silicon carbide by attenuated total reflection of mid-IR radiation. Reflectance measurements demonstrate critical coupling by a double scan of wavelength and incidence angle. Critical coupling occurs when prism coupling loss is equal to losses in silicon carbide and the substrate, resulting in maximal electric field enhancement. © 2009 Optical Society of America

*OCIS codes:* 240.5420, 160.1245.

Surface plasmon/phonon-polaritons (SPPs) are electromagnetic waves confined to the interface between polaritonic ($\epsilon_p<0$) and dielectric ($\epsilon_d>0$) materials. Negative $\epsilon$ can result from collective oscillations of conduction electrons in metals (plasmons) [1,2] or lattice vibrations (phonons) in polar crystals such as ZnSe, SiC, and InP [3]. Because of their tight confinement to the metal/dielectric interface and their sensitivity to $\epsilon_d$, surface *plasmon*-polaritons have long been employed for ultrasensitive index sensing using visible light, e.g., for detecting adsorption of atomic-layer films [4]. Extending this sensitive technique into the mid-IR has great potential in spectroscopic "fingerprint" identification but has not been widely implemented. In addition to sensing [5], mid-IR SPPs find applications that include near-field superlensing [6], highly efficient thermal emission [7], and surface wave particle acceleration [8].

It is impossible to directly couple light to SPPs, because their propagation wavenumber, $k_{\mathrm{SPP}}$ [given by Eq. (1)] implies that $k_{\mathrm{SPP}}>\omega/c$, where $\omega\equiv 2\pi c/\lambda$ and $\lambda$ is the vacuum wavelength of light. Therefore, auxiliary coupling devices such as gratings or high-index prisms are necessary [1]. When a prism is used, either Otto [9] [the focus of this Letter: see the inset of Fig. 3(d) for a schematic] or Kretschmann configurations are employed. Regardless of the coupling approach, it is desirable to couple all or most of the incident radiation into SPPs. The complete coupling of laser energy to SPPs—*critical coupling*—results in vanishing reflectivity and the largest enhancement of the SPP field over the incident laser field $E_0$.

The main result of this Letter is that, by using SiC films grown on a Si substrate, we theoretically describe and experimentally demonstrate critical coupling to SPPs. We solve the dispersion relation for the complex propagation constant $k_{\mathrm{free}}$ of a leaky and lossy SPP and demonstrate that critical coupling is achieved when the energy loss of the *free* SPP into the prism is equal to the sum of all other losses (resistive loss and substrate leakage). Finally, by conducting a double scan of incident angle $\theta$ and wavelength $\lambda$ for two air gaps, we experimentally demonstrate critical coupling to SPPs between the prism and the SiC film. SPPs are launched using evanescent light coupling in the Otto configuration, and their presence is measured by attenuated total reflection (ATR) of $p$-polarized (TM) radiation. Theoretically, for every wavelength, there exists a small gap $d_{\mathrm{gap}}$ (typically $<10$ $\mu$m) and an incidence angle $\theta_0$ for which reflectivity $R(\lambda_0,\theta_0,d_{\mathrm{gap}})=0$, corresponding to critical coupling. In practice, $R=0$ is unattainable because of the finite angular beam spread. Therefore, we experimentally deduce critical coupling from the global minimum of $R(\lambda,\theta)$ for each $d_{\mathrm{gap}}$. While the excitation of mid-IR SPPs has been measured by scanning $\lambda$ [10,11], *critical coupling* to SPPs—which requires a double scan in $(\lambda,\theta)$—has not been experimentally demonstrated to our knowledge.

To review, SPP and prism dispersion relations are

$$k_{\mathrm{SPP}}=\frac{\omega}{c}\sqrt{\frac{\epsilon_{\mathrm{SiC}}\epsilon_0}{\epsilon_{\mathrm{SiC}}+\epsilon_0}},\quad k_x=\frac{\omega}{c}\sqrt{\epsilon_{\mathrm{ZnSe}}}\sin\theta,\qquad(1)$$

where $k_{\mathrm{SPP}}$ describes dispersion at the semi-infinite air/SiC interface and $k_x$ describes the prism dispersion light line. For air, $\epsilon_0=1$, and the standard equation for polar crystals describes SiC permittivity:

$$\epsilon_{\mathrm{SiC}}(\omega)=\epsilon_\infty\frac{\omega^2-\omega_{\mathrm{LO}}^2+i\gamma\omega}{\omega^2-\omega_{\mathrm{TO}}^2+i\gamma\omega},\qquad(2)$$

where $\omega_{\mathrm{LO}}=972$ cm$^{-1}$ ($\lambda_{\mathrm{LO}}=10.288$ $\mu$m), $\omega_{\mathrm{TO}}=796$ cm$^{-1}$ ($\lambda_{\mathrm{TO}}=12.563$ $\mu$m), $\gamma=3.75$ cm$^{-1}$, and $\epsilon_\infty=6.5$ fit $T$ and $R$ data for a 1.5 $\mu$m air-bridged membrane (characterization details are provided elsewhere [12]). Strong evanescent coupling to SPPs through the high-index ZnSe hemisphere ($\epsilon_{\mathrm{ZnSe}}=5.76$) occurs when $k_x\approx\mathrm{Re}(k_{\mathrm{SPP}})$. The SPP dispersion curve $\omega(k_{\mathrm{SPP}})$ and prism light lines $\omega(k_x)$ are shown in Fig. 1, satisfying excitation criteria where intersecting. This simple argument is merely qualitative, because (i) it does not account for the finite thickness of SiC or SPP's leakage into the Si substrate, (ii) the

0146-9592/09/172667-3/$15.00 

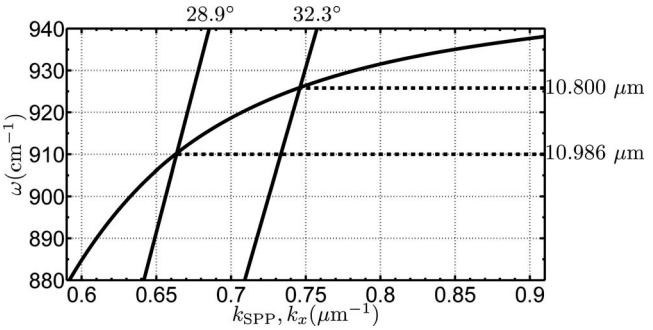


Fig. 1. Dispersion curves corresponding to Eq. (1): $k_{SPP}$ (curved line) and $k_x$ (two straight lines for the two $\theta$'s indicated above, corresponding to the two critical coupling cases). Light lines ($k_x$) intersect $k_{SPP}$ at two frequencies: $\lambda = 10.800\ \mu$m and $\lambda = 10.986\ \mu$m (inaccessible to $CO_2$ laser).

prism's proximity is not taken into account, and (iii) SPP's excitation efficiency is not quantified.

To circumvent these three limitations, we numerically solved the dispersion relation for a free SPP propagating along the air/SiC interface of a ZnSe/air/SiC/Si system, accounting for (i) and (ii). Energy radiates into ZnSe and Si, contributing to the SPP energy loss. We calculated the complex propagation constant $k_{free}(\omega) = k_{res} + i\kappa$, where $k_{res} \approx k_{SPP}$ and $\kappa = \kappa_{ohm}^{SiC} + \kappa_{rad}^{Si} + \kappa_{rad}^{ZnSe}$ (in the limit of weak loss). The $\kappa$'s are spatial decay rates: $\kappa_{ohm}^{SiC}$ represents ohmic loss in SiC, and $\kappa_{rad}^{Si}$ and $\kappa_{rad}^{ZnSe}$ represent radiative leakage into Si and ZnSe, respectively. Matching the incident laser beam's $k_x$ to $k_{res}$ excites resonant SPPs. For weak loss, free SPP leakage into ZnSe is equivalent to laser-driven SPP coupling from ZnSe.

For laser-driven SPPs, reflectivity is given by the Lorentzian response

$$R = 1 - \frac{4(\kappa_{ohm}^{SiC} + \kappa_{rad}^{Si})\kappa_{rad}^{ZnSe}}{(k_x - k_{res})^2 + (\kappa_{ohm}^{SiC} + \kappa_{rad}^{Si} + \kappa_{rad}^{ZnSe})^2} \qquad (3)$$

in the limit of weak loss and when $\theta$ is such that $k_x \approx k_{res}$. A derivation of a similar response for a three-layer plasmonic system can be found in [1].

Zero reflectivity (critical coupling) occurs when $\kappa_{rad}^{ZnSe} = \kappa_{ohm}^{SiC} + \kappa_{rad}^{Si}$. Of course, any solution of the dispersion relation for a fixed frequency yields only a single decay rate $\kappa$. Separate $\kappa_{rad}^{ZnSe}$ and $\kappa_{ohm}^{SiC} + \kappa_{rad}^{Si}$ can then be extracted by varying $d_{gap}$ and by recognizing that for large $d_{gap}$, radiative loss into ZnSe vanishes, resulting in $\kappa = \kappa_{ohm}^{SiC} + \kappa_{rad}^{Si}$. Thus, to find the correct gap for critical coupling, we vary $d_{gap}$ until the imaginary part of $k_{free}$ is twice its value for large gaps: $\kappa(d) = 2\kappa(d = \infty)$. According to Eq. (3), this specific gap $d_{gap}(\lambda_0)$ corresponds to critical coupling. $\kappa(d)$ is shown in Fig. 2(a) for two different frequencies, enabling the identification of critical coupling gaps $d_{1,2}$. Next, the laser-driven solution is obtained as a function of $\theta$ for $d_{1,2}$ by assuming light incident from the ZnSe side. As shown in Fig. 2(b), reflectivity indeed vanishes for $d_{1,2}$, corresponding to critical coupling.

To experimentally demonstrate critical coupling, we used ATR measurements to detect SPPs excited in

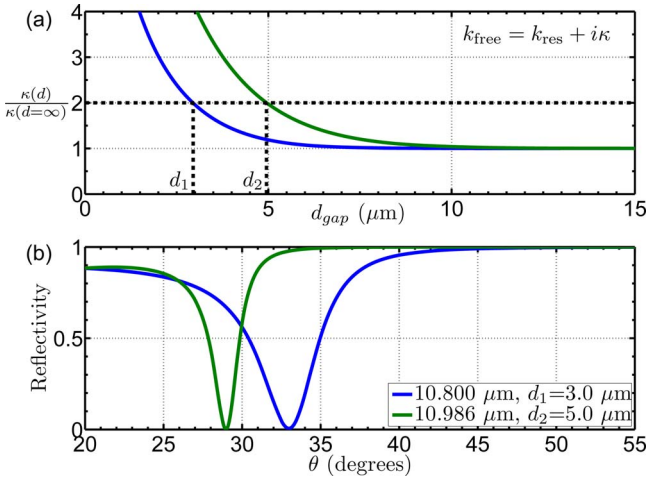


Fig. 2. (Color online) (a) $\kappa(d)$ (the imaginary part of $k_{free}$) is normalized to $\kappa(d = \infty)$ ($k_{free}$ is SPP in-plane wave vector). Critical coupling occurs when coupling loss into the prism ($\kappa_{rad}^{ZnSe}$) is equal to losses in SiC ($\kappa_{ohm}^{SiC}$) and the Si substrate ($\kappa_{rad}^{Si}$), shown graphically as $\kappa(d) = 2\kappa(d = \infty)$. (b) Reflectivity $R$ versus $\theta$ is plotted for two driven SPPs, each with an air gap satisfying critical coupling criterium. $\kappa(d = \infty) = \kappa_{ohm}^{SiC} + \kappa_{rad}^{Si} = 22$ and $10\ \text{mm}^{-1}$ for $\lambda_{1,2} = 10.800$ and $10.986\ \mu$m, respectively.

the Otto configuration, as shown in the Fig. 3(d) inset. Growth of the $1.5\ \mu$m 3C-SiC film on a Si(100) substrate was achieved with a two-step atmospheric pressure chemical vapor deposition: substrate carbonization under propane at 1150 °C was followed by epitaxial growth using a silane/propane mixture at 1350 °C [13]. The growth rate was $3\ \mu$m/h. IR radiation from a line-tunable cw $^{13}CO_2$ laser was coupled through a 2.5 cm ZnSe prism, aligned in close proximity to SiC to allow for finite air gaps. Incident and reflected radiation was measured using a laser power meter (5% accuracy). A rotation stage provided angular steps of 0.5°. Gap distance was determined *in situ* by HeNe laser (632.8 nm) interferometry (50 nm accuracy). Two air gaps were used: $d_1 = 3\ \mu$m and $d_2 = 5\ \mu$m. Laser tunability ranges are 10.666–10.867 $\mu$m (R branch) and 11.025–11.310 $\mu$m (P branch).

In our first experiment, we measured reflection spectra for $d_2 = 5\ \mu$m, shown in Fig. 3(a). Note that experimental reflectivity $R$ never falls below 30%, and that $R$ reaches its minimum at the boundaries of the laser tunability ranges. This implies that critical coupling for $d_2$ is never achieved because the corresponding $\lambda_2$ is not accessible to the laser. The physical interpretation is that for the laser's P branch, long-range SPPs are overcoupled (coupling from ZnSe greater than other losses), whereas for the R branch, short-range SPPs are undercoupled (coupling from ZnSe less than other losses).

Numerical simulations shown in Fig. 3(b) confirm these conclusions: $\lambda_2 = 10.986\ \mu$m corresponding to critical coupling is outside of the two available laser frequency branches. Numerical results are averaged assuming a Gaussian angular profile (2° FWHM) that best matches the experimental apparatus. Note that, according to the simulations and Eq. (3), the

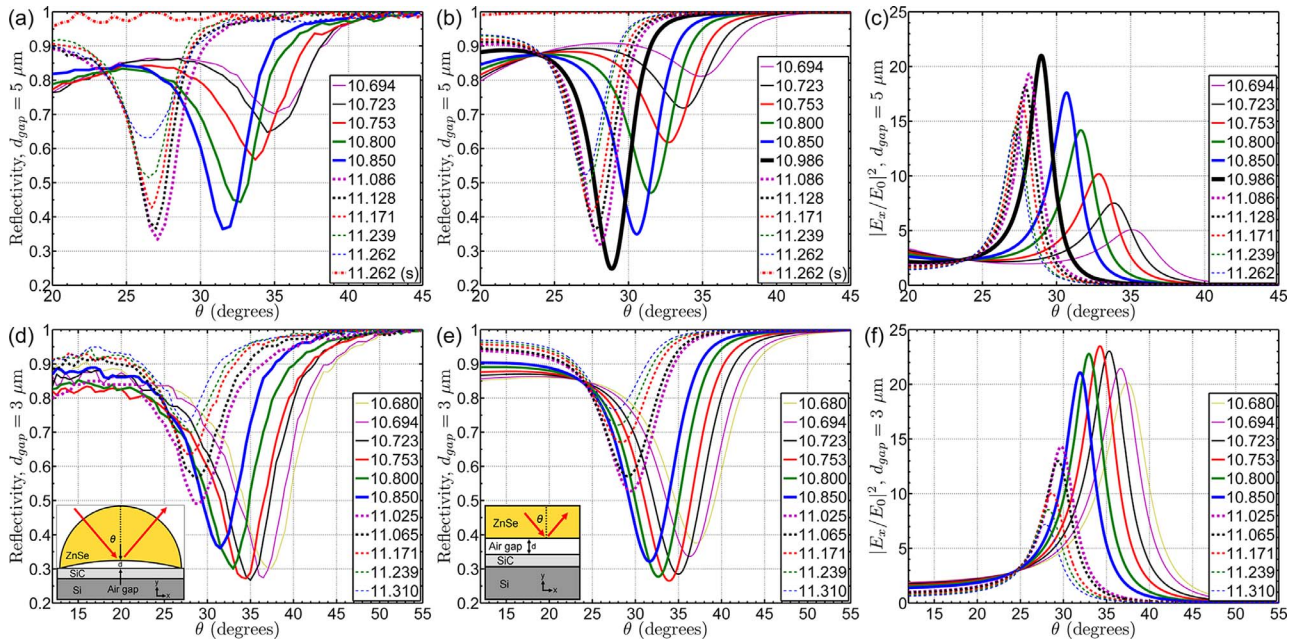


Fig. 3. (Color online) Top panel: (a) experimental and (b) theoretical plots of laser reflectivity versus $\theta$, with the $s$-polarized (TE) reflectivity included, and (c) theoretical field enhancement $|E_x/E_0|^2$ in the plane of SiC (Otto configuration, $d=5\ \mu$m air gap). Critical coupling was not observed for this gap because of laser tunability limitations, but the trend toward criticality is clear and is predicted for $\lambda_2=10.986\ \mu$m [shown in (b) and (c)]. Bottom panel: same for the reduced air gap $d_1=3\ \mu$m. (d) Experimental and (e) theoretical reflectivities with corresponding setup schematics insets (not to scale) and (f) field enhancement $|E_x/E_0|^2$. Theoretical reflections and field enhancements are averaged over a finite angular spread to model the experimental conditions.

finite angular spread prevents $R$ from vanishing even for $\lambda=\lambda_2$. However, the global minimum of $R(\lambda_2,\theta_2)$ shown in Fig. 3(b) clearly indicates critical coupling, which would be experimentally achievable with greater $\lambda$ tunability. Simulations also show that critical coupling to SPPs is accompanied by the strongest electric field enhancement [1]. Figure 3(c) displays calculated field enhancement $|E_x/E_0|^2$ at the SiC/air interface, with a maximum value of 21.0 at critical coupling.

To achieve critical coupling, we reduced the gap to $d_1=3\ \mu$m and double scanned $R(\lambda,\theta)$, shown in Fig. 3(d). The global reflectivity minimum at $\lambda_1^{exp}=10.753\ \mu$m agrees with numerical simulations shown in Fig. 3(e), within the 5% experimental error. Plane wave (zero angular spread) calculations shown in Fig. 2(b) predict critical coupling at $\lambda_1=10.800\ \mu$m. If angular divergence is reduced by a factor of 2.2, the experimentally measurable global minimum of $R$ would indeed shift from $\lambda_1^{exp}$ to $\lambda_1$.

In conclusion, we have presented what we believe to be the first experimental demonstration of critical coupling to mid-IR SPPs at the air/SiC interface in the Otto configuration. Critical coupling was observed by performing a double scan of wavelength and incidence angle for two air gaps. We have theoretically shown that critical coupling occurs when prism coupling is equal to other SPP losses. Because critical coupling results in the largest field enhancement, mid-IR index-sensing applications are envisioned.

This work was supported by the National Science Foundation (NSF) NIRT grant 0709323 and the U.S. Airforce Office of Scientific Research (AFOSR) MURI grants FA9550-06-1-0279 and FA9550-08-1-0394.

## References

1. H. Raether, *Surface Plasmons on Smooth and Rough Surfaces and on Gratings* (Springer-Verlag, 1988).
2. W. L. Barnes, A. Dereux, and T. W. Ebbesen, Nature **424**, 824 (2003).
3. R. Hillenbrand, T. Taubner, and F. Keilmann, Nature **418**, 159 (2002).
4. J. Giergiel, C. Reed, S. Ushioda, and J. Hemminger, Phys. Rev. B **31**, 3323 (1985).
5. A. Ganjoo, H. Jain, C. Yu, J. Irudayaraj, and C. Pantano, J. Non-Cryst. Solids **354**, 2757 (2008).
6. T. Taubner, D. Korobkin, Y. Urzhumov, G. Shvets, and R. Hillenbrand, Science **313**, 1595 (2006).
7. J.-J. Greffet, R. Carminati, K. Joulain, J.-P. Mulet, S. Mainguy, and Y. Chen, Nature **416**, 61 (2002).
8. S. Kalmykov, O. Polomarov, D. Korobkin, J. Otwinowski, J. Power, and G. Shvets, Philos. Trans. R. Soc. London Ser. A **364**, 725 (2006).
9. A. Otto, Z. Phys. **216**, 398 (1968).
10. D.-Z. A. Chen and G. Chen, Appl. Phys. Lett. **91**, 121906 (2007).
11. N. Kuroda, Y. Iida, T. Shigeta, H. Watanabe, and J. Watanabe, Jpn. J. Appl. Phys. Part 1 **42**, L1241 (2003).
12. Y. A. Urzhumov, D. Korobkin, B. Neuner III, C. Zorman, and G. Shvets, J. Opt. A **9**, S322 (2007).
13. M. J. Hernandez, G. Ferro, T. Chassagne, J. Dazord, and Y. Monteil, J. Cryst. Growth **253**, 95 (2003).